Journal of Pharmacology and Toxicology

ISSN 1816-496X

Academic Journals Inc.

www.academicjournals.com

Journal of Pharmacology and Toxicology 1 (5): 456-463, 2006
ISSN 1816-496X

Molecular Modelling Analysis of the Metabolism of Ibuprofen

Fazlul Huq
School of Biomedical Sciences, Faculty of Health Sciences,
The University of Sydney, Australia

Abstract: Molecular modelling analyses based on molecular mechanics, semi-empirical (PM3) and DFT (at B3LYP/6-31G* level) calculations show that there are both electron-rich and electron-deficient regions on the molecular surfaces of IBF and its metabolites so that they can be subject to both electrophilic and nucleophilic attacks. The latter attack means that they can react with cellular glutathione, thus causing glutathione depletion and hence oxidative stress, and can also cause oxidation of nucleobases in DNA and thus DNA damage. However, the large LUMO-HOMO energy differences observed for IBF and all its metabolites may mean that the rates of such adverse reactions may be low.

Key words: Ibruprofen, NSAID, arthritis, toxicity, glutathione, molecular modelling

Introduction

Ibuprofen (IBP, 2-(4-isobutylphenyl)propanoic acid) is a non-steroidal anti-inflammatory drug (NSAID) that is widely used in humans and veterinary medicine in the treatment of acute and chronic rheumatoid arthritis (Rorarius *et al*., 1993). It is the drug of choice among the 'profen' class of NSAIDs because of its low unwanted side effects (Hao *et al*., 2005). It is also used as a paediatric anti-inflammatory agent (Bennet *et al*., 1992).

IBP is a chiral molecule that can exist in R- and S-configurations. Metabolic chiral inversion is actually a common characteristic of other arylpropanoic derivatives such as ketoprofen, flubiprofen and pranoprofen (Hao *et al*. 2005). It is believed this metabolic activation of IBF through chiral inversion not only leads to higher therapeutic potency but may also cause a greater risk of acute kidney failure in patients with renal disorders (Marasco *et al*., 1987). The adverse effects of IBF include gastrointestinal disturbances and central nervous system depression; however, the severity is found to be mild (McElwee *et al*., 1990).

The metabolism of IBF in man involves conjugation with glucuronic acid to form ibuprofen acylglucuronide (IBF-GLU) which is stereoselective to *S*-enantiomer (Lee *et al*., 1985), oxidation to produce two major metabolites, 2-hydroxyibuprofen (2HIBF) and carboxyibuprofen (CIBF) (Adams *et al*., 1967; Mills *et al*., 1973; Brooks and Gilbert 1974; Kaiser *et al*., 1976; Paterson *et al*., 1978). The urinary excretion of free IBF, IBF-GLU, 2HIBF and CIBF accounts for between 74 to 86% of an oral dose following the administration of the racemic mixture to man. Three other minor oxidation products: 1-hydroxibuprofen (1HIBF), 3-hydroxyibuprofen (3HIBF) and 2-(4-carboxyphenyl) propanoic acid (CPPA) have also been identified in human urine. The formation of possible metabolite 2-(4-hydroxymethylphenyl) propanoic acid (HPPA) remains speculative as it has not been detected. CYP2C9 is the predominant enzyme responsible for the oxidative metabolism of IBF as it is true for any other NSAIDs (Tracy *et al*. 1995). Figure 1 shows the metabolic pathway of IBF in humans.

In this study, molecular modelling analyses have been carried out using the program Spartan '02 (2002) to investigate the relative stability of IBF and its metabolites with the aim of providing a better understanding on their relative toxicity. The study was carried out in the School of Biomedical Sciences, The University of Sydney during January to June 2006.

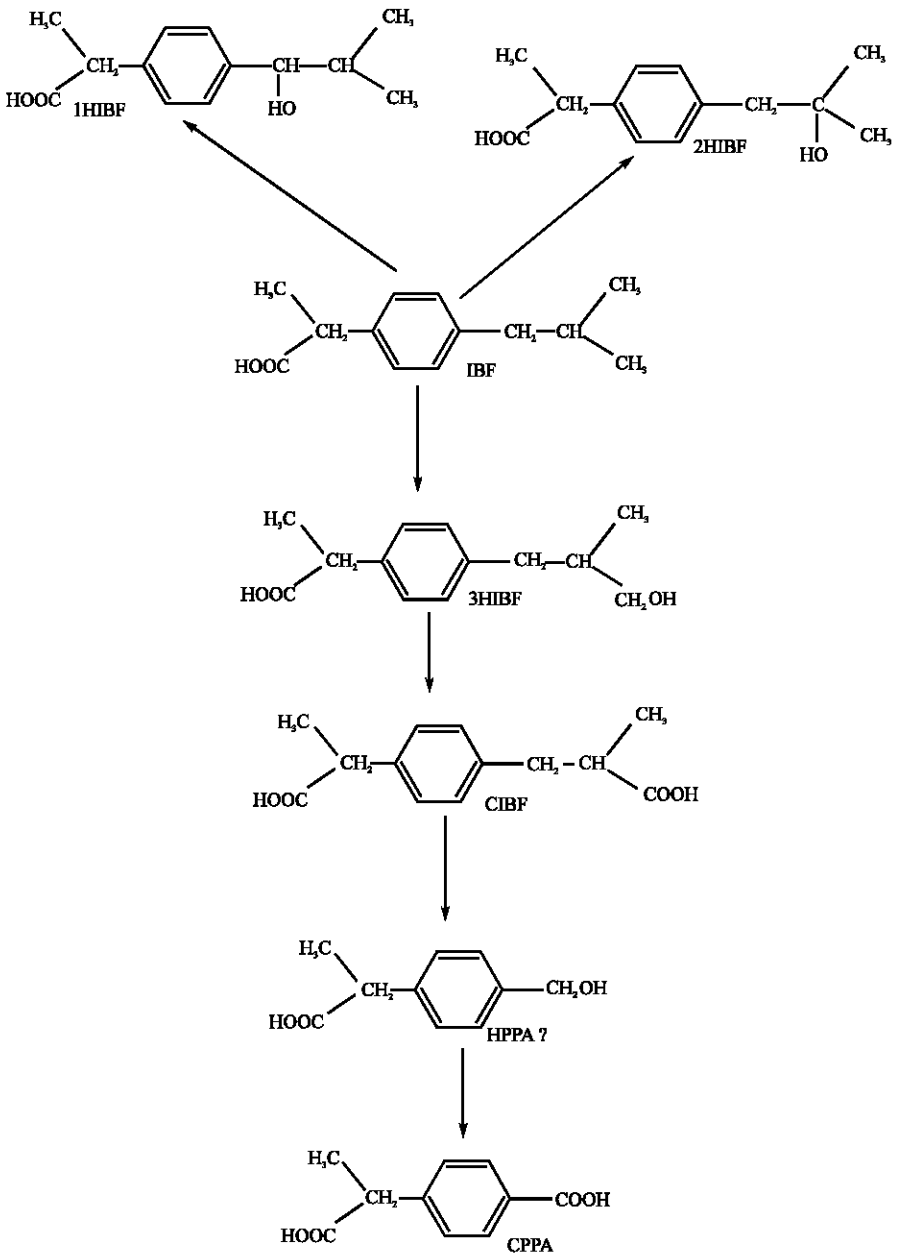

Fig. 1: Metabolic pathways for ibuprofen (Tan *et al*., 2002) - HPPA has not been detected

Materials and Methods

The geometries of ibuprofen and its metabolites have been optimised based on molecular mechanics, semi-empirical and DFT calculations, using the molecular modelling program Spartan '02. Molecular mechanics calculations were carried out using MMFF force field. Semi-empirical calculations were carried out using the routine PM3. DFT calculations were carried at B3LYP/6-31G* level. In optimization calculations, a RMS gradient of 0.001 was set as the terminating condition. For the

optimised structures, single point calculations were carried out to give heat of formation, enthalpy, entropy, free energy, dipole moment, solvation energy, energies for HOMO and LUMO. The order of calculations: molecular mechanics followed by semi-empirical followed by DFT ensured that the structure was not embedded in a local minimum. To further check whether the global minimum was reached, some calculations were carried out with improvable structures. It was found that when the stated order was followed, structure corresponding to the global minimum or close to that could ultimately be reached in all cases. Although RMS gradient of 0.001 may not be sufficiently low for vibrational analysis, it is believed to be sufficient for calculations associated with electronic energy levels.

Results and Discussion

Table 1 gives the total energy, heat of formation as per PM3 calculation, enthalpy, entropy, free energy, surface area, volume, dipole moment, energies of HOMO and LUMO as per both PM3 and DFT calculations for IBF and its metabolites 1HIBF, 2HIBF, 3HIBF, CIBF, HPPA and CPPA. Figure 2-8 give the regions of negative electrostatic potential (greyish-white envelopes) in (a), HOMOs (where red indicates HOMOs with high electron density) in (b), LUMOs in (c), and density of surface charges (where red indicates negative, blue indicates positive and green indicates neutral) in (d) as applied to the optimised structures of IBF and its metabolites 1HIBF, 2HIBF, 3HIBF, CIBF, HPPA and CPPA.

The calculated solvation energies of IBF and its metabolites 1HIBF, 2HIBF, 3HIBF, CIBF, HPPA and CPPA from PM3 calculations in kcal mol^{-1} are, respectively -7.99, -10.55, -10.68, -13.41, -19.18, -14.89 and -19.23 and their dipole moments from DFT calculations are 4.9, 3.5, 6.5, 6.0, 4.2. 4.8 and 2.8, respectively. The values suggest metabolites of IBF would be more soluble in water than the parent drug so that they are more readily excreted via urine. CIBF and CPPA would be most soluble in water and hence most easily excreted.

IBF and its metabolites are found to have large LUMO-HOMO energy differences (that range from 5.50 to 6.61 eV from DFT calculations), indicating that IBF and all its metabolites would be kinetically inert. The relative ease in excretion via urine and the kinetic inertness may explain why the toxic side effects from IBF therapy are found to be low.

In the case of IBF, CIBF and CPPA, the electrostatic potential is found to be more negative around carboxyl oxygen atoms, indicating that the positions may be subject to electrophilic attacks. In the case of 1HIBF, 2HIBF, 3HIBF and HPPA, the electrostatic potential is found to be more negative around carboxyl and hydroxyl oxygen atoms, once again indicating that the positions may be subject to electrophilic attacks.

Table 1: Calculated thermodynamic and other parameters of ibuprofen and its metabolites

Molecule	Calculation type	Total energy (kcal mol^{-1}/ atomic unit*)	Heat of formation (kcal mol^{-1})	Enthalpy (kcal mol^{-1} K^{-1})	Entropy (cal mol^{-1} K^{-1})	Solvation energy (kcal mol^{-1} K^{-1})	Free energy (kcal mol^{-1})	Area (Å^2)	Volume (Å^3)	Dipole moment (debye)	Homo (eV)	Lumo (eV)	Lumo-Homo (eV)
IBF	PM3	-106.89	-98.90	187.64	125.05	-7.99	150.36	254.95	234.28	4.7	-9.69	-0.16	9.53
	DFT	-656.70		188.49	124.67	-9.23	151.33	260.39	236.60	4.9	-6.64	-0.49	6.15
1HIBF	PM3	-146.83	-136.28	190.82	132.19	-10.55	151.41	266.35	242.84	3.2	-10.01	-0.41	9.60
	DFT	-731.91		191.63	131.77	-11.89	152.36	267.50	243.89	3.5	-6.72	-0.61	6.11
2HIBF	PM3	-150.20	-139.52	191.15	132.36	-10.68	151.68	265.85	242.67	6.2	-9.76	-0.18	9.58
	DFT	-731.91		191.99	131.67	-12.07	152.75	267.46	243.76	6.5	-6.57	-0.41	6.16
3HIBF	PM3	-151.82	-138.41	191.24	129.72	-13.41	152.57	262.38	241.44	5.7	-9.73	-0.20	9.53
	DFT	-731.90		192.05	130.33	-14.93	153.21	268.11	243.92	6.0	-6.58	-0.44	6.14
CIBF	PM3	-197.68	-178.50	180.28	137.21	-19.18	139.37	270.29	245.25	4.7	-10.11	-0.51	9.60
	DFT	-805.94		181.05	136.76	-21.14	140.30	271.50	246.31	4.2	-6.88	-0.72	6.16
HPPA	PM3	-137.97	-123.08	135.73	112.52	-14.89	102.18	209.43	188.03	4.1	-9.99	-0.46	9.53
	DFT	-613.96		136.44	113.15	-15.91	102.72	210.66	188.78	4.8	-6.80	-0.70	6.10
CPPA	PM3	-181.06	-161.81	125.29	116.41	-19.23	90.58	214.17	190.89	3.7	-10.57	-1.01	9.56
	DFT	-688.00		126.15	115.79	-20.76	91.64	212.51	191.12	2.8	-7.32	-1.82	5.50

* in atomic units from DFT calculations

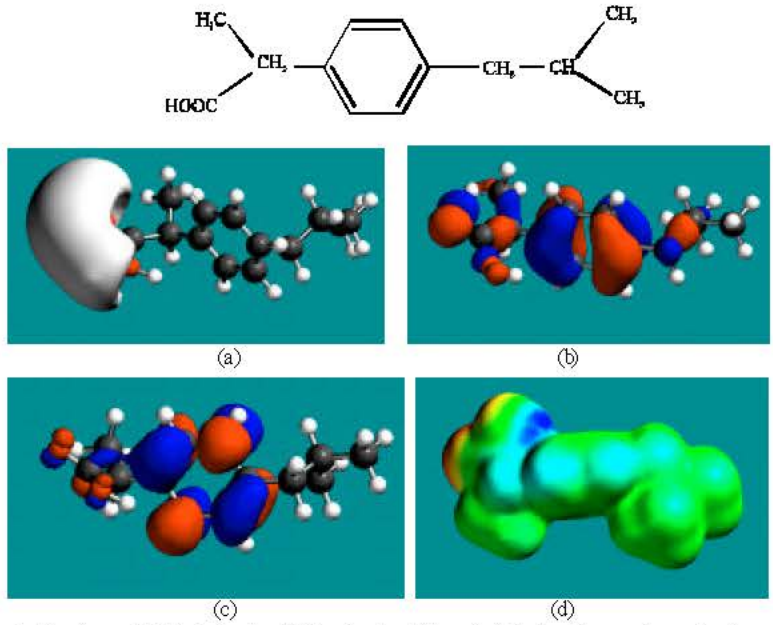

Fig. 2: Structure of IBF giving in: (a) the electrostatic potential (greyish envelope denotes negative electrostatic potential), (b) the HOMOs, (where red indicates HOMOs with high electron density) (c) the LUMOs (where blue indicates LUMOs) and in (d) density of electrostatic potential on the molecular surface (where red indicates negative, blue indicates positive and green indicates neutral)

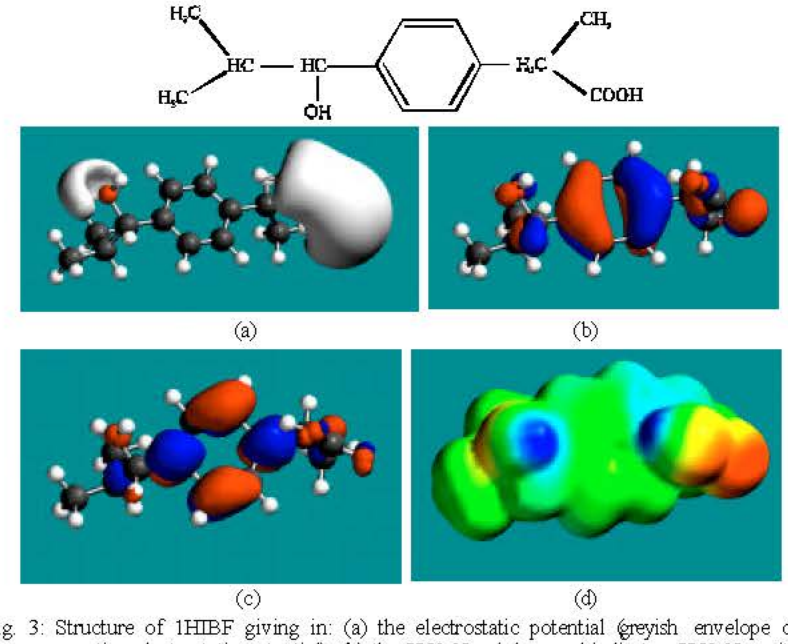

Fig. 3: Structure of 1HIBF giving in: (a) the electrostatic potential (greyish envelope denotes negative electrostatic potential), (b) the HOMOs, (where red indicates HOMOs with high electron density) (c) the LUMOs (where blue indicates LUMOs) and in (d) surface electric charges (where red indicates negative, blue indicates positive and green indicates neutral)

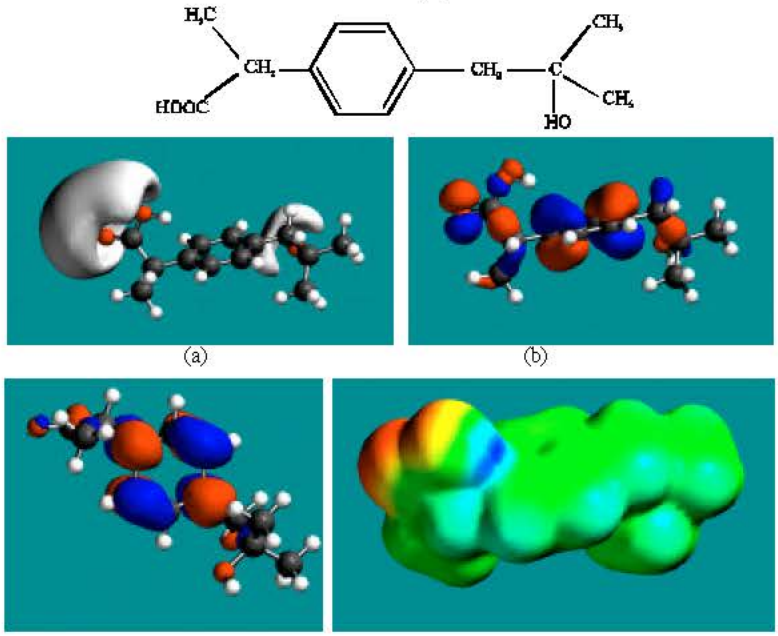

Fig. 4: Structure of 2HIBF giving in: (a) the electrostatic potential (greyish envelope denotes negative electrostatic potential), (b) the HOMOs, (where red indicates HOMOs with high electron density) (c) the LUMOs (where blue indicates LUMOs) and in (d) surface electric charges (where red indicates negative, blue indicates positive and green indicates neutral)

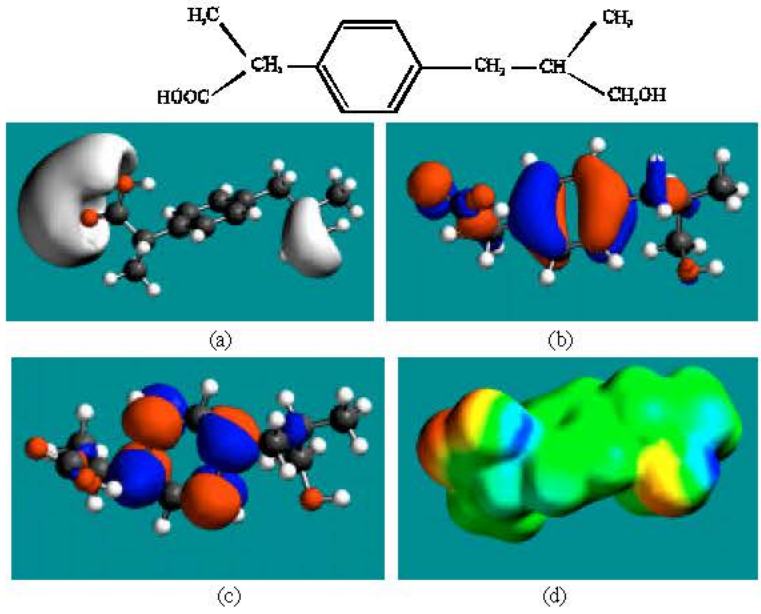

Fig. 5: Structure of 3HIBF giving in: (a) the electrostatic potential (greyish envelope denotes negative electrostatic potential), (b) the HOMOs, (where red indicates HOMOs with high electron density) (c) the LUMOs (where blue indicates LUMOs) and in (d) surface electric charges (where red indicates negative, blue indicates positive and green indicates neutral)

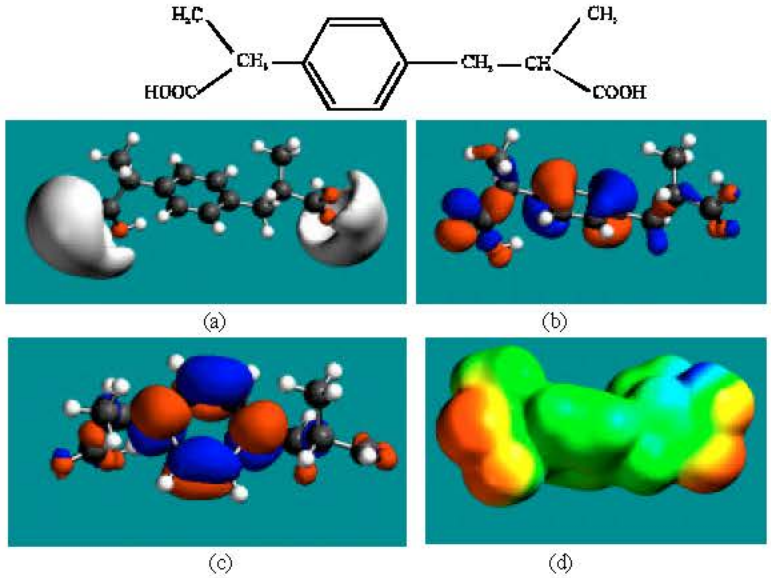

Fig. 6: Structure of CIBF giving in: (a) the electrostatic potential (greyish envelope denotes negative electrostatic potential), (b) the HOMOs, (where red indicates HOMOs with high electron density) (c) the LUMOs (where blue indicates LUMOs) and in (d) surface electric charges (where red indicates negative, blue indicates positive and green indicates neutral)

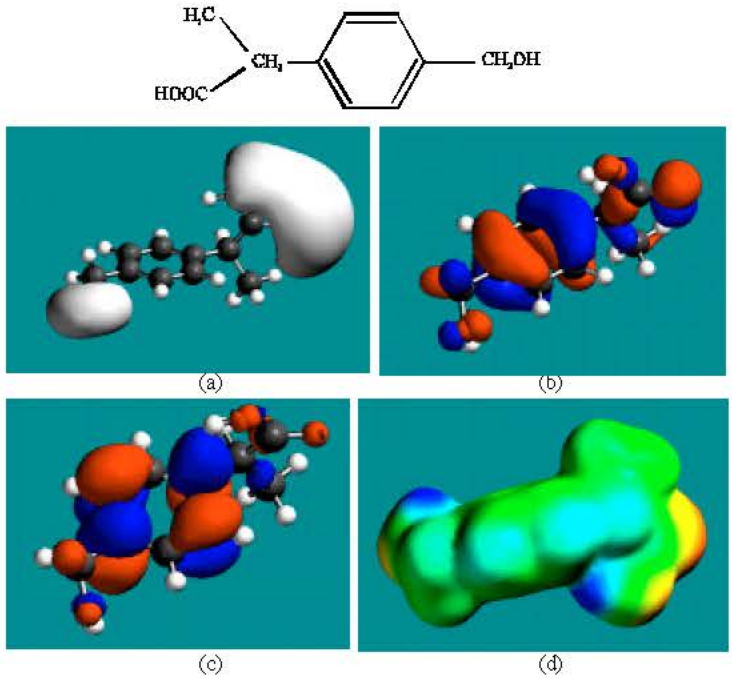

Fig. 7: Structure of HPPA giving in: (a) the electrostatic potential (greyish envelope denotes negative electrostatic potential), (b) the HOMOs, (where red indicates HOMOs with high electron density) (c) the LUMOs (where blue indicates LUMOs) and in (d) surface electric charges (where red indicates negative, blue indicates positive and green indicates neutral)

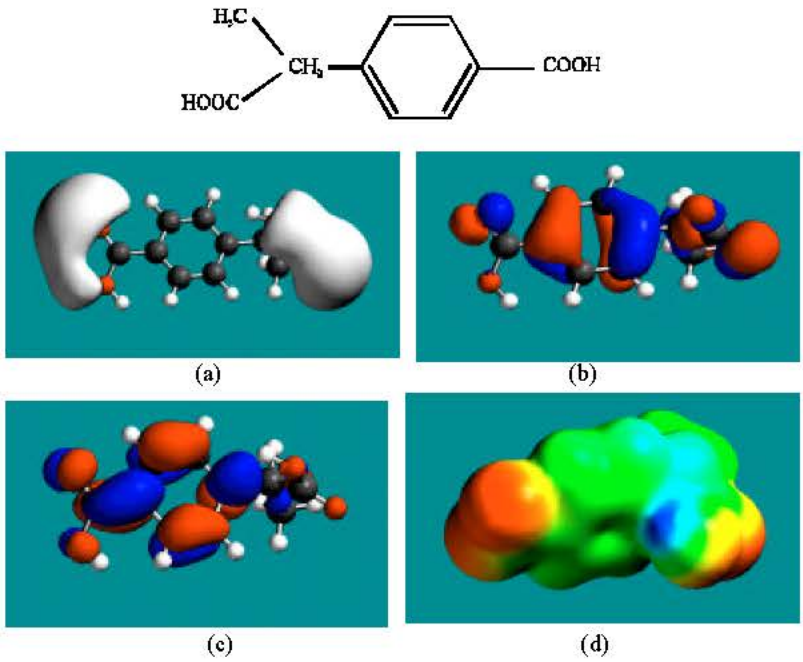

Fig. 8: Structure of CPPA giving in: (a) the electrostatic potential (greyish envelope denotes negative electrostatic potential), (b) the HOMOs, (where red indicates HOMOs with high electron density) (c) the LUMOs (where blue indicates LUMOs) and in (d) surface electric charges (where red indicates negative, blue indicates positive and green indicates neutral)

In the case of IBF, 1HIBF, 2HIBF and 3HIBF, HOMOs with high electron density are found close to most of the non-hydrogen atoms except the two methyl carbon atoms of the isobutyl moiety whereas the LUMOs are found to concentrate on the non-hydrogen atoms of propanoic acid moiety and phenyl ring. In the case of CIBF, HPPA and CPPA both HOMOs with high electron density and LUMOs are found close to most of the non-hydrogen atoms.

The overlap or close proximity of positions of HOMOs with high electron density and those of negative electrostatic potential give further support to the idea that the positions may be subject to electrophilic attacks. When the electron densities on molecular surfaces (Fig. 2d to 8d) are considered, it can be seen that the molecular surfaces of IBF and all its metabolites, have both electron-rich and electron-deficient regions so that they may be subject to both electrophilic and nucleophilic attacks. The latter attack means that IBF and its metabolites can react with cellular glutathione and can oxidize nucleobases in DNA. Reaction with glutathione introduces oxidative stress by compromising the anti-oxidant status of the cell whereas oxidation of nucleobses in DNA causes DNA damage. However, as stated earlier IBF and its metabolites are expected to be kinetically inert so that the rates of such adverse reactions would be low.

Conclusions

Molecular modelling analyses based on molecular mechanics, semi-empirical (PM3) and DFT (at B3LYP/6-31G* level) calculations show that there are some electron-deficient regions on the molecular surfaces of IBF and its metabolites so that they can react with cellular glutathione, thus causing glutathione depletion and hence oxidative stress, and can also cause oxidation of nucleobases in DNA

and hence DNA damage. However, the large LUMO-HOMO energy differences observed for IBF and all its metabolites may mean that the rates of such adverse reactions may be low. Thus the mild toxicity associated with the drug IBF may be explained in terms of kinetic inertness and ease in excretion.

Acknowledgments

The author is grateful to the School of Biomedical Sciences, The University of Sydney for the time release from teaching.

References

Adams, S.S., E.E. Cliffe, B. Lassel and J.S. Nicholson, 1967. Biological properties of 2-(4-isobutylphenyl)-propionic acid. J. Pharmaceut. Sci., 56: 1686.

Bennett, M.J., W.G. Sherwood, A. Bhala and D.E. Hale, 1992. Identification of urinary metabolites (+/-)-2-(p-isobutylphenyl)propionic acid (ibuprofen) by routine organic acid screening. Clin. Chim. Acta, 210: 55-62.

Brooks, C.J.W. and M.T. Gilbert, 1974. Studies of urinary metabolites of 2-(4-isobutylphenyl)propionic acid by gas-liquid chromatography-mass spectrometry. J. Chromatogr., 99: 541-460.

Hao, H., G. Wang and J. Sun, 2005. Enantioselective pharmacokinetics of ibuprofen and involved mechanisms. Drug Metabol. Rev., 1: 215-234.

Kaiser, D.G., G.J. Van Giessen, R.J. Reischer and W.J. Wechter, 1976. Isomeric inversion of ibuprofen (*R*)-enantiomer in humans. J. Pharm. Sci., 65: 269-273.

Lee, E.J.D., K. Williams, R. Day and G. Graham, 1985. Stereoselective disposition of ibuprofen enantiomers in man. Br. J. Clin. Pharmacol., 19: 669-674.

Marasco, W.A., P.W. Gikas, R. Azziz-Baumgartner, R. Hyzy, C.J. Eldredge and J. Stross, 1987. Ibuprofen-associated renal dysfunction. Pathophysiologic mechanisms of acute renal failure, hyperkalemia, tubular necrosis, and proteinuria. Arch. Intl. Med., 147: 2107-2116.

McElwee, N.E., J.C. Veltri, D.C. Bradford and D.E. Rollins, 1990. A prospective, population-based study of acute ibuprofen overdose: complications are rare and routine serum levels not warranted. Ann. Emerg. Med., 19: 657-662.

Mills, R.F.N., S.S. Adams, E.E. Cliffe, W. Dickinson and J.S. Nicholson, 1973. The metabolism of ibuprofen. Xenobiotica, 3: 589-598.

Patterson, J.E., G.A. Ulsakker and E. Jellum, 1978. Studies on the metabolism of 2,4'-isobutylphenylpropionic acid (ibuprofen) by gas chromatography and mass spectrometry. Dialysis fluid, a convenient medium for studies on drug metabolism. J. Chromatogr., 528: 413-420.

Rorarius, M.G., P. Suominen, G.A. Baer, O. Romppanen and R. Tuimala, 1993. Diclofenac and ketoprofen for pain treatment after elective caesarean section. Br. J. Anaesth., 70: 293-297.

Spartan '02 2002. Wavefunction, Inc. Irvine, CA, USA.

Tan, S.C., B.K. Patel, S.H.D. Jackson, C.G. Swift and A.J. Hutt, 2002. Stereoselectivity of ibuprofen metabolism and pharmacokinetics following the administration of the racemate to healthy volunteers. Xenobiotica, 32: 683-697.

Tracy, T.S., B.W. Rosenbluth, S.A. Wrighton, F.J. Gonzalez and K.R. Korzekwa, 1995. Role of cytochrome P450 2C9 and allelic variant in the 4'-hydroxylation of (R)- and (S)-flurbiprofen. Biochem. Pharmacol., 49: 1269-1275.